Protease inhibitors block apoptosis at intermediate stages: a compared analysis of DNA fragmentation and apoptotic nuclear morphology

L. Ghibelli[a,*], V. Maresca[a], S. Coppola[a], G. Gualandi[b]

[a]*Dipartimento di Biologia, Università di Roma Tor Vergata, via della Ricerca Scientifica, 00123 Roma, Italy*
[b]*DABAC, Università della Tuscia, 01100 Viterbo, Italy*

Received 3 October 1995

Abstract The possible correlation between DNA digestion and changes in nuclear morphology in apoptosis was studied by blocking the apoptotic process at intermediate stages. The apoptogenic action of three drugs: etoposide, puromycin, tributyltin, was contrasted with protease inhibitors with different specificity on U937 cells. The inhibitors interfered with the development of the apoptotic features without shifting cell death to necrosis: treated cells showed abnormal morphologies, which could be recognized as intermediate stages of apoptosis; accordingly, DNA analysis showed an inhibitor-dependent block of the apoptotic DNA digestion. The comparison between size of DNA fragments and nuclear morphology suggested the following correlations: loss of normal nuclear shape with the appearence of a ≥2 Mb DNA band; ongoing chromatin condensation with the progressive DNA digestion up to 50 kb; nuclear fragmentation with DNA laddering. Protease inhibitors in etoposide-treated cells did not allow the formation of 700–300 kb fragments, suggesting that they possibly derive from a cell-mediated effect.

Key words: Apoptosis; Proteases inhibitor; DNA digestion; Nuclear morphology; Etoposide

1. Introduction

Specific proteolytic events have been found to be involved in the process of apoptosis induced by many different stimuli. The Interleukin converting enzyme (ICE protease [1]), as well as proteases present in cytotoxic granules [2,3], when introduced and/or activated in the cell, are able to induce apoptosis; complementary, apoptosis may be blocked by specific protease inhibitors [4]. While most proteins maintain their integrity in the apoptotic cells, several specific proteins have been shown to be proteolitically digested in apoptosis, such as nuclear lamins [5–7], fodrin [8], histone H1 [9], poly(ADP-ribose)polymerase [5,10]. Some of the proteases involved in apoptosis have been identified, such as calpain, a Ca^{2+}-dependent cystein protease involved in cytoskeletal alterations (i.e. blebbing) [11]; a novel 24 kDa serine protease involved in the activation of the nuclease-dependent DNA digestion [12]; a protease involved in Fas-induced apoptosis [13].

*Corresponding author. Fax: (39) (6) 202 3500.

Abbreviations: Mb, megabases; kb, kilobases; HMW, high molecular weight; FCS, foetal calf serum; PMC, puromycin; TBT, tributyltin; VP16, etoposide; TI, soy-bean trypsin inhibitor; PMSF, phenyl-methyl-sulphonyl-fluoride; IAA, iodoacetamide; NEM, *N*-ethyl-maleimide; TLCK: Na-*p*-tosyl-L-lysine chloromethyl ketone; TPCK, *N*-tosyl-L-phenylalanine chloromethyl ketone.

The execution of the apoptotic process implies a chain of events which leads to the full development of the apoptotic features, such as DNA digestion into fragments of 200 base pairs and multiples (ladder), and nuclear fragmentation in several membrane-bound vesicles [14,15].

DNA laddering is the final result of the progressive digestion of the cell genome carried on by several endonucleases [16]. They probably act following a hyerarchical order, producing at first well defined classes of High Molecular Weight (HMW) DNA fragments (300 and 50 kb), by a process dependent on proteolytic events [17], which may involve topoisomerases [18]. Later, DNA is further cleaved into the ladder. DNA digestion is not completed in some cell systems, intermediate stages being thus detectable [19]: in these instances a DNA ladder is not found, and the 50 kb fragments are instead accumulated.

Also the changes in nuclear morphology are the result of a precise progression of events, implying in most instances the complete condensation of cell chromatin and its budding from the nuclear envelope [20]. This process is not completed in some cell systems, intermediate stages being thus detectable: in these instances masses of condensed chromatin in the form of crescents are located just within the nuclear envelope, without budding [21].

A precise correlation between biochemical and morphological events in apoptosis has not yet been made: the intermediate stages, which would help to analyze this correlation, are very unfrequent among cells induced to apoptosis, because the whole process is very rapid and starts asincronously [22], whatever the inducer. In this study, we used protease inhibitors to block the apoptotic process at intermediate stages with the aim of correlating the events leading to nuclear fragmentation with those leading to chromatin digestion.

2. Materials and methods

2.1. Cell culture and treatments

U937 cells were cultured in RPMI 1640 medium supplemented with 10% FCS, 2 mM L-glutamine, 100 IU/ml penicillin and streptomycin), and kept in a controlled atmosphere (5% CO_2) incubator at 37°C. Cell viability has been assessed by Trypan blue exclusion. Induction to apoptosis: incubation for 4 h with: 10 μg/ml PMC; 1 μg/ml TBT; 100 μg/ml VP16. Proteases inhibition: the inhibitors were added just before the apoptogenic treatment, and kept throughout the experiment (none of the inhibitors was cytotoxic within 24 h) at the following doses: TI, 100 μg/ml; PMSF, 1 mM; IAA, 10 μM; NEM, 10 μM; TLCK, 50 μg/ml; TPCK, 50 μg/ml.

2.2. Analysis and quantification of cell morphology and apoptosis

At the end of each treatment, 2×10^5 cells were resuspended and fixed in 4% paraformaldeide, loaded on a gelatinized slide, stained with hematoxylin, and analyzed by direct optical microscopy. Apoptosis has been quantified by counting at least 100 cells in at least 3 random selected fields [23]. The abundance of each morphological class was

SSDI 0014-5793(95)01284-2

then estimated by counting at least 300 cells in at least 10 random selected fields.

2.3. Analysis of DNA ladder

2×10^6 cells were lysed in a buffer containing 10 mM EDTA, 100 mM Tris pH 8, 0.5% Sodium Lauroyl Sarkosine, 200 μg/ml proteinase K. Nucleic acids were extracted by phenol-(chloroform/isoamylic alcohol 24:1), ethanol precipitated, incubated in 100 μg/ml RNAse A 60′ at 37°C. The purified DNA from 2×10^6 was loaded on a 1.5% agarose gel in TAE buffer, stained with 10 μg/ml ethydium bromide, and visualized on a 254 nM UV transilluminator.

2.4. Pulsed field gel electrophoresis

In the preparation of agarose plug, 10^6 cells were processed as described in [17]. Contour-clamped homogeneous electric field (CHEF) gel electrophoresis was carried out using the 'Gel Navigator' horizontal chamber and 'Pulsaphor' 2015 controller. Total run time was 19 h at 180 V and 9° C. In particular: 180-s pulses for 4 h, 90-s pulses for 6 h, 45-s pulses for 5 h and 20-s pulses for 4 h.

3. Results

3.1. Kinetics of VP16, PMC, TBT induced apoptosis

Here described is the analysis of the apoptogenic action of three drugs acting on different cellular targets: etoposide (VP16), which inhbit topoisomerase II by stabilyzing the cleavable complex [24], puromycin (PMC), which blocks protein synthesis by interfering with elongation [25], tributyltin (TBT), which interferes with protein, DNA and cytoskeleton structure [26]. These inducers have been chosen because they act on different targets, thus presumably inducing apoptosis with a different mechanism; moreover, apoptosis occurs rapidly and massively, concerning ≥ 60% of cells within four hours (Fig. 1), so that at the end of the treatment the apoptotic cells have not yet degenerated. The full apoptotic morphology of U937 implies a strong cell blebbing and a heavy nuclear fragmentation, independently of the inducer. At early times of treatment, cells with abnormal morphologies are detected, albeit rarely: these cells recalls the intermediate stages of apoptosis as detected by ultrastructural analysis (Dini et al., submitted); they are quite rare, suggesting a very rapid evolution toward the final apoptotic morphology.

3.2. Cells with intermediate apoptotic morphologies are detected upon apoptogenic treatments in the presence of protease inhibitors

A set of protease inhibitors with different specificities has been tested on U937; the doses have been chosen as the highest which did not alter cell viability within 24 h and not induce any gross morphological alterations. The presence of protease inhibitors during the apoptogenic treatments, reduced the extent of drug-induced apoptosis (Table 1). This was not due to a shift to cell death by necrosis, as monitored by the Trypan blue exclusion test (Table 1): instead, at the end of treatment (4 h), the intermediate stages of apoptosis became very abundant, as though an inhibitor-dependent accumulation had occurred. Longer treatments allowed a small fraction of the intermediate stages to evolve into full apoptosis, while most cells remained frozen at the early steps: this suggests that protease inhibitors acted to block some apoptotic steps rather than slowing down the whole process.

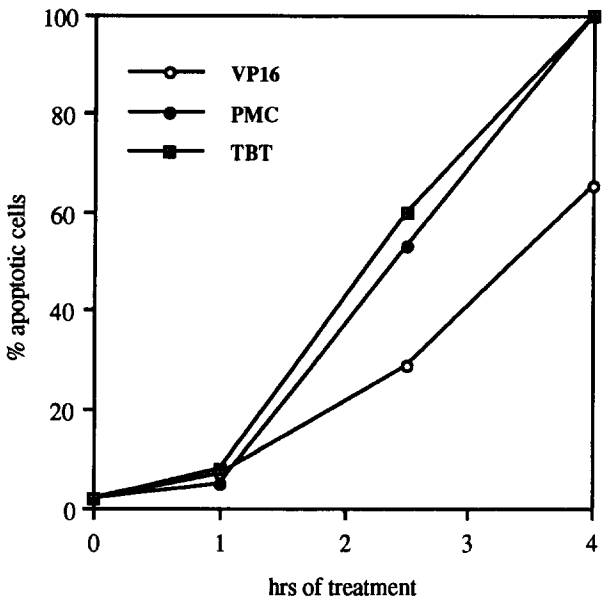

Fig. 1. Kinetics of apoptosis. Apoptosis induced on U937 by VP16, PMC, TBT, has been quantified according to [23]. A typical experiments is shown among three (TBT) and > 10 (VP16 and PMC) performed. While TMT and PMC has an identical kinetics, VP16 is a slower inducer.

3.3. Progression through intermediate stages of apoptosis

A transmission electron microscopy analysis of U937 induced to apoptosis upon many treatments allowed to describe a progression of events from normal to fully apoptotic cells (Dini et al., submitted), which is graphycally depicted in panel A of Fig. 2: normal cells, with relaxed chromatin and irregularly shaped nuclei (stage I); the nuclei loose the irregular shape becoming rounded, though maintaining the chromatin relaxed (stage II); then chromatin condenses progressively in patches at the nuclear edge (stage III); the patches bud from the nuceus to give fully apoptotic cells with fragmented nuclei (stage IV).

The features considered in the present analysis are only those which can be unambigously detected by optical microscopy

Table 1
Quantification of apoptotic and trypan blue excluding cells in the presence of protease inhibitors

% Apoptotic cells (% trypan blue excluding)	Inducer only	+NEM	+IAA	+PMSF	+T.I.	+TLCK	+TPCK
VP16	66 (97)	4 (92)	2 (99)	48 (97)	58 (99)	28 (88)	3 (92)
PMC	83 (99)	8 (99)	19 (88)	45 (95)	90 (99)	31 (99)	2 (89)
TBT	86 (99)	9 (74)	21 (80)	67 (56)	84 (80)	82 (64)	3 (96)

Apoptosis induced on U937 by VP16, PMC, TBT, in the presence of protease inhibitors, has been quantified according to [23]. In parentheses is the fraction of cells excluding trypan blue at the end of the treatment. One experiment (among > 5 performed) is shown, the same that has been analyzed for the DNA patterns.

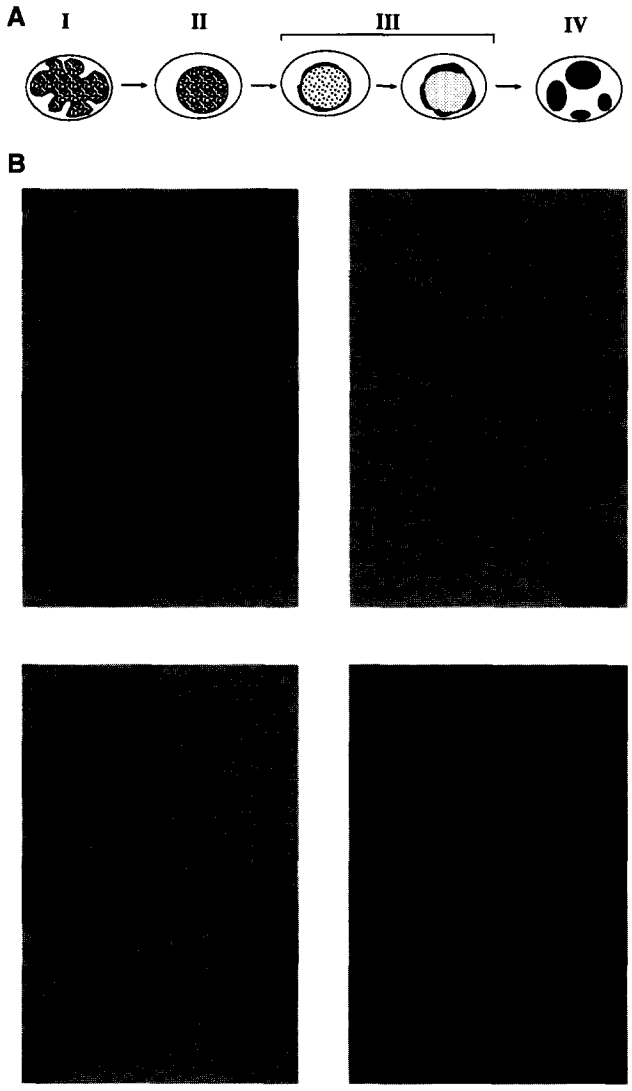

Fig. 2. Progression from viable cells to apoptotic cells. (A) The drawing illustrates the progession to apoptosis as results from the electron microscopy analysis of U937 induced to apoptosis (Dini et al., submitted). (B) Morphologies of U937 induced to apoptosis in the presence of protease inhibitors. (a) untreated cells: see the irregularly shaped nuclei (stage I); (b) PMC + TPCK: see most of the cells with rounded, sharply defined nuclei and non-condensed chromatin (stage II); (c) PMC + NEM; see cells with chromatin progressively condensing at the nuclear edge, at an early (empty arrow) and late (dark arrow) stage III; (d) PMC alone: see apoptotic cells with fragmented nuclei and compact chromatin (stage IV).

upon nuclear staining, such as nuclear shape and gross chromatin condensation. According to these criteria, the abnormal morphologies detected upon apoptogenic treatments in the presence of protease inhibitors resemble the intermediate stages II and III. As an example, panel B of Fig. 2 shows untreated U937 (a) and U937 induced to apoptosis by PMC in the presence of TPCK (b), NEM (c), and without protease inhibitors (d). The resemblance of cells in c with stage II, cells in d with early (empty arrows) and late (dark arrows) stage III, allows to hypothesize that a progression of events toward apoptosis has been inhibited by different protease inhibitors at different stages.

3.4. *Quantitative analysis of cells at intermediate stages of apoptosis*

A quantitative analysis of the morphologies shown in Fig. 2 has been performed for all apoptogenic treatments in the presence of all protease inhibitors; Fig. 3 shows the results, as the fraction of cells belonging to each of the four categories (experiments with VP16 and PMC; TBT behavior overlaps that of PMC, with the difference that TLCK did not alter TBT's apoptogenic action, see Table 1). Upon VP16 treatment, a total (NEM) or partial but substantial (TLCK and IAA) rescue to perfectly normal cell morphology was found (Fig. 3a). This was not found upon PMC or TBT treatments (Fig. 3b): thus, TPCK, TLCK and IAA may block a very early step in VP16-induced apoptosis, which is not shared by TBT or PMC; alternatively, they may inhibit a pre-apoptotic signalling event in response to the direct VP16-induced DNA cleavage (see below).

The most striking effect is observed, upon all three apoptogenic treatments, with TPCK (Fig. 3a and b): most cells show a normally relaxed chromatin but have lost the normal, irregular nuclear shape, becoming rounded (stage II vs. stage I, see Fig. 2). This suggests that a first step towards apoptosis has been made, but TPCK has tightly blocked a function which is necessary in order to proceed to the next step (i.e. chromatin condensation).

Cells with chromatin condensed at the nuclear periphery, without nuclear fragmentation (stage III: see Fig. 2) are also accumulated, mostly upon inhibition of cystein proteases (NEM and IAA, see Fig. 3). These cells, even though their chromatin has condensed, are not undergoing nuclear fragmentation, suggesting that cystein proteases have a role in nuclear fragmentation.

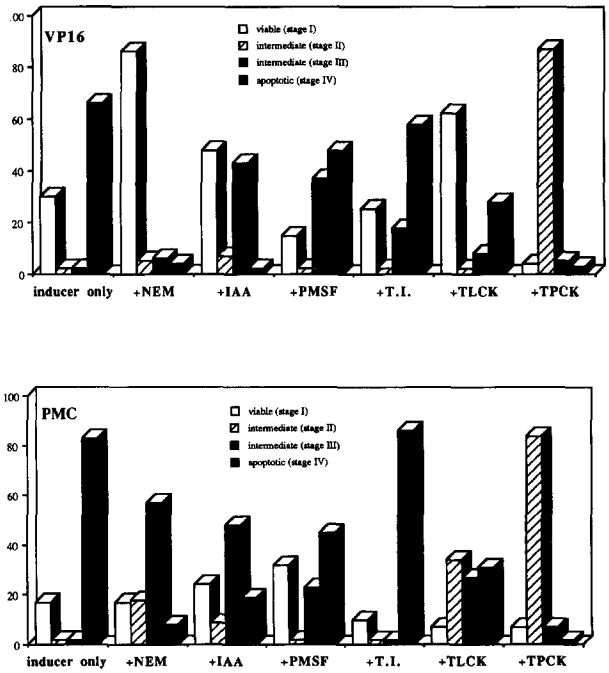

Fig. 3. Quantitative analysis of cells with normal, apoptotic and intermediate morphologies. The different morphologies have been quantified at four hrs of treatment, as described in materials and methods. The results show one experiment among four performed. Bars' values indicate the percentage of cells showing the corresponding morphology.

3.5. *Apoptotic DNA degradation is blocked at different stages by protease inhibitors*

PFGE analysis (Fig. 4a) shows that healthy U937 cells have only intact DNA, unable to enter the gel (lane C). Cells induced to apoptosis by VP16 have many classes of fragments: bands at ≥2 Mb, 1.3 Mb, 700, 300, and 48 kb (indicated by the closed triangles in Fig. 4a, VP16, lanes '0'), and a smear of < 50 kb. Upon PMC and TBT treatments, only the 2Mb and 48kb band and the lower smear are clearly detectable, while the others are very faint (closed triangles in Fig. 4a, PMC lanes '0'; the pattern obtained with TBT is identical with the exception that TLCK did not inhibit apoptotic DNA digestion). The degree of DNA digestion is reduced by all protease inhibitors but tripsin inhibitor. Strikingly, upon all apoptogenic treatments, in the presence of TPCK (lane 7 on Fig. 4a and b) DNA is cleaved to form the ≥2 Mb band, whereas any further digestion into smaller molecules is inhibited.

In the presence of cystein protease inhibitors (NEM and IAA), the whole set of fragments up to 50 kb are formed, while the smear of lower fragments (corresponding to the DNA ladder) is very faint: the nuclease responsible for ladder formation seems thus not working.

DNA from treated cells has also been analyzed by conventional electrophoresis on 1.2% agarose gel. A DNA ladder has been found in all treatments which led to the < 50 kb smear, thus confirming PFGE analysis. Fig. 4b shows the DNA pattern upon four exemplificative treatments, the same which have been shown in Fig. 2B to induce four different morphological types: PMC alone (lane 0); PMC + NEM; PMC + TPCK; control cells: a ladder is clear in PMC, very faint or undetectable in the presence of NEM and TPCK.

The comparison between DNA digestion and nuclear morphological changes in apoptosis upon protease inhibition suggests that cells at stage II have the DNA cleaved up to the ≥2 Mb band, while cells at stage III show the DNA HMW fragments but not the DNA ladder; fully apoptotic cells (stage IV) show nuclear fragmentation and DNA ladder; no exception is found by comparing data in Fig. 2 with Fig. 4. The clearest observations in support to this correlations are the following: TPCK in all apoptogenic treatments blocked the progression of DNA digestion at the ≥2 Mb band (Fig. 4a and b), concomitantly blocking chromatin condensation (Fig. 2); NEM and IAA accumulated cells at stage III and inhibited DNA laddering but not HMW fragments formation; TLCK on PMC lead to the presence of cells at stage II, III and IV, and the DNA pattern show fragments of any size, from ≥2 Mb up to the DNA ladder.

3.6. *VP16-induced DNA fragmentation in 700–300 kb is probably cell-mediated*

The 2Mb band, by the conditions used in the PFGE analysis described here, is the result of the accumulation of fragments measuring ≥2 Mb (i.e. PFGE protocols more suitable for very large DNA fragments might allow to resolve it into more bands). This band, which is very intense upon VP16 treatments (Fig. 4a), may originate, in addition to the early apoptotic digestion, also from the DNA damage caused directly by VP16. In the presence of TPCK (lane 7) and NEM (lane 2), no molecules smaller than 2 Mb are detectable: since the inhibitors block the DNA cleavage in 700 and 300 kb HMW fragments, it is likely that these fragments do not originate from the DNA damage caused directly by VP16 action on topoisomerase II, but are instead mediated by a further cellular function.

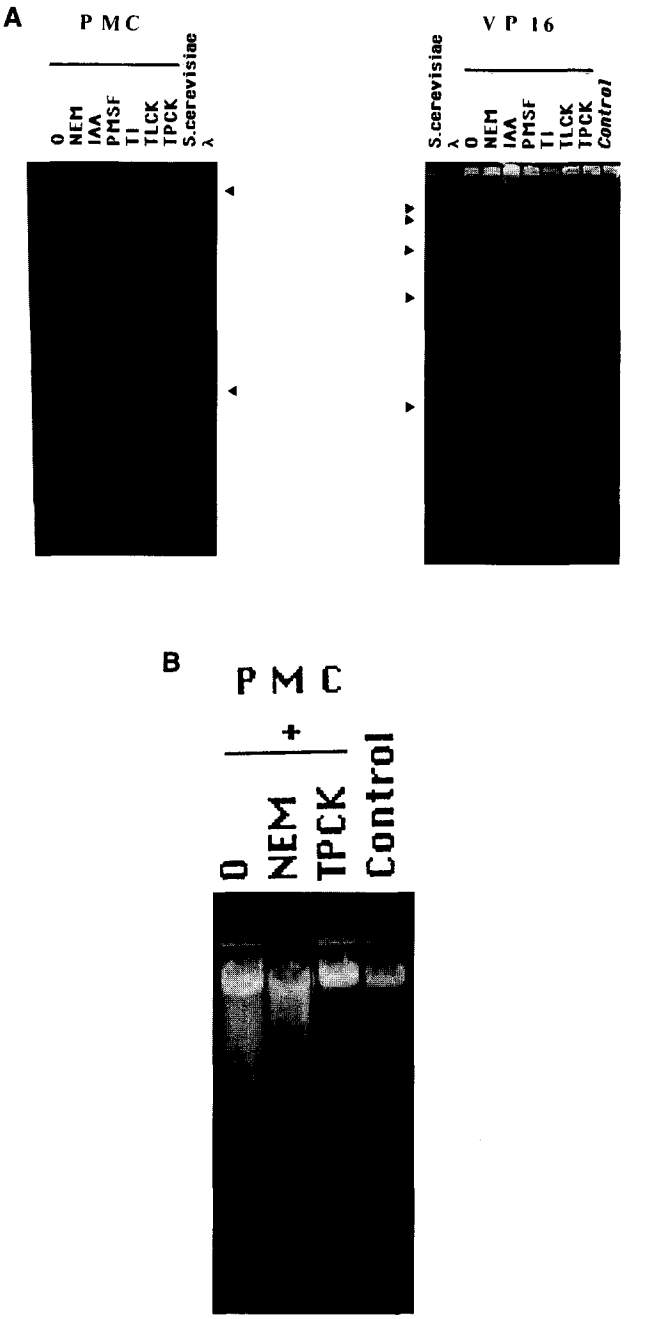

Fig. 4. DNA analysis. The results from one experiment is shown among two complete experiments performed. (A) Pulsed field gel electrophoresis analysis: closed triangles indicate the bands resulting from DNA digestion upon treatments with inducer only, as described in the text (0 = inducer only; *S. cerevisiae*: commercially available size marker spanning from 2200 to 225 kb; λ = undigested λ genome, 50 kb). (B) Conventional agarose gel electrophoresis. Analysis of DNA ladder upon induction to apoptosis with protease inhibitors: exemplificative treatments giving a significant difference among each other are shown.

4. Discussion

Before discussing the results, some preliminary considera-

tions may help to define the scope of this study. The experiments have been performed on living cells: this did not allow the use of the specific but cell-unpermeable peptide-based protease inhibitors; moreover, the doses of the less specific cell-permeable inhibitors had to be kept below toxicity, and might then be not sufficient for a complete enzymatic inhibition: thus TPCK, which could be used at high concentrations, tightly blocked the progression of apoptosis, while NEM or IAA, necessarily used at very low concentrations, lead to 'leaky' blocks. The presence of a tight block may have obscured the presence of a second block at a downstream step. In our system, serine and cystein protease inhibitors in some instances produced overlapping effects; on the other hand, serine proteases exerted effects which differed among each other (i.e. compare TPCK and PMSF): this may be explained because each inhibitor acts on its own set of enzymes, and overlapping effects are to be expected. Some difference in the behavior of protease inhibitors on the three apoptogenic treatments (i.e. NEM rescued to healthy cell morphology VP16 treated cells, while blocking PMC and TBT treated cells at stage III) might be due to a difference in the mechanism of induction to apoptosis. The same may apply for the different pattern of HMW fragments in PMC and TBT vs. VP16 treated cells, since only the latter showed the 1300, 700 and 300 kb bands.

The present study was aimed to analyze the correlation between the morphological changes occurring in the nuclei of apoptotic cells and the progression of DNA digestion, which was allowed by the finding that protease inhibitors induced the accumulation of cells at intermediate stages of apoptosis. This is in line with the concept of apoptosis as a 'programmed' chain of interdependent events occurring in a defined temporal sequence, and not a catastrophic process. While the involvement of proteases in apoptotic DNA digestion has been clearly assessed [12,17], a similar approach to nuclear morphology is lacking so far. The comparison between size of DNA fragments and nuclear morphology allowed to establish a 'temporal' association between nuclear and DNA changes occurring in apoptosis: the loss of normal nuclear shape with the appearence of a $\geq$2Megabases DNA band; ongoing chromatin condensation with the progressive DNA digestion up to 50 kb; nuclear fragmentation with DNA laddering. Though clear, these correlations have been obtained by using not very specific protease inhibitors, which may interfere with other cellular functions unrelated to proteolysis (i.e. NEM is a powerful thiol alkylating agent): thus, it would be interesting to challange these correlations with more natural events. A 'naturally occurring' accumulation at intermediate stages has been reported in hepatocytes treated with TGF1β [21]: chromatin condenses in the absence of nuclear fragmentation, and no DNA ladder is detectable. Other findings describe that nuclear fragmentation can occur also in the absence of a DNA ladder in epithelial [19] and lymphoid cells ([27] and M. Marini, personal communication): systems not so 'well equipped' for apoptosis as U937 cells, may lack the functions (enzymes?) necessary to undergo some of the late events in apoptosis (i.e. absence of DNAse I [7]).

A possible link between the apoptotic changes in nuclear morphology and DNA digestion is the fate of the nuclear lamins, which have been found to be proteolytically degraded in apoptosis [5–7]: the analysis of the function of nuclear lamins in healthy cells suggests that lamin breakdown could be involved in both nuclear re-shaping and apoptotic chromatin fragmentation. Nuclear lamins digestion has indeed been shown to occur both at the beginning and during apoptosis, being probably involved in chromatin condensation [28]

VP16 induces two types of DNA cleavage in whole cells: direcly by the stabilization the cleavable complexes created by topoisomerase II; and indirectly by the activation of the apoptotic nucleases. DNA fragments of 700 and 300 kb are detected by PFGE in in vivo (whole cell) experiments soon after VP16 exposure: they are believed to be a direct effect of the drug-enzyme interaction and not a sign of ongoin apoptosis, because they form also when apoptosis is inhibited (i.e. by actinomycin D, [24]) and reseal upon drug removal (while apoptosis is irreversible [29]). In our system, TPCK and NEM inhibit the formation of the 700 and 300 kb fragments: this (unless both TPCK and NEM directly block topoisomerase II before the formation of the cleavable complex, thereby eliminating VP16 target) suggests that they are not the direct effect of VP16 cleavage, but the result of a cell-mediated response to VP16, an early signalling event which stops when the drug is removed. The nature of the unknown signalling event which triggers apoptosis in response to VP16-induced DNA damage, hypthesized by many authors, might be a proteolysis: indeed, NEM, and partially IAA and TLCK, which inhibited VP16 apoptogenic action ab initio both at the morphological and DNA level, may have interfered with such early signalling.

Acknowledgements: V.M. is a recipient of a fellowship from 'Scuola di Specializzazione in Biotecnologie' by Montedison, whose grant has supported the cost of this research.

References

[1] Miura, M., Zhu, H., Rotello, R., Hartwieg, E.A., Yuan, J. (1993) Cell 75, 653–660.
[2] Shi, L., Kam, C.M., Powers, J.C., Aebersold, R., Greenberg, A.H. (1992) J. Exp. Med. 176, 1521–1529.
[3] Shi, L., Kraut, R.P., Aebersold, R., Greenberg, A.H. (1992) J. Exp. Med. 175, 553–566.
[4] Sarin, A., Adams, D.H., Henkart, P.A. (1993) J. Exp. Med. 178, 1693–1700.
[5] Kaufmann, S.H. (1989) Cancer Res. 49, 5870–5878.
[6] Lazebnik, Y.A., Cole, S., Cooke, C.A., Nelson, W.G., Earnshow, W.C. (1993) J. Cell Biol. 123, 7–22.
[7] Ucker, D.S., Obermiller, P.S., Eckart, W., Apger, J.R., Berger, N.A., Meyers, J. (1992) Mol. Cell Biol. 12, 3060–3069.
[8] Martin, S.J., O'Brien, G.A., Nishioka, W.K., McGahon, A.J., Mahboubi, A., Saido, T.C., Gree, D.R. (1995) J.Biol. Chem. 270, 6425–6428.
[9] Gaziev, A.I., Kutsyi, M.P. (1992) Int. J. Radiat. Biol. 61, pp. 169–174.
[10] Kaufmann, S.H., Desnoyers, S., Ottaviano, Y., Davidson,.E., Poirier, G.G. (1993) Cancer Res. 53, 3976–3985;.
[11] Squier, M.K., Miller, A.C., Malkinson, A.M., Cohen, J.J. (1994) J. Cell Physiol. 159, 229–237.
[12] Wright, S.C., Wei, Q.S., Zhong, J., Zheng, H., Kinder, D.H., Larrick, J.W. (1994) J. Exp. Med. 180, 2113–2123.
[13] Schlegel, J., Peters, I., Orrenius, S. (1995) FEBS Lett. 364, 139–142.
[14] Wyllie, A.H. (1987) J. Pathol. 153, 313–316.
[15] Wyllie, A.H. (1980) Nature 284, 555–558.
[16] Peitsch, M.C., Mannherz, H.G., Tschopp, J. (1994) Trends Cell Biol. 4, 37–41.
[17] Zhivotovsky, B., Wade, D., Gahm, A., Orrenius, S., Nicotera, P. (1994) FEBS Lett. 351, 150–154.
[18] Kataoka, A., Kubota, M., Wakazono, Y., Okuda, A., Bessho, R., Wei Lin, Y., Usami, I., Akyiama, Y., Furusho, K. 1995 FEBS Lett. 364, 264–267.
[19] Oberhammer, F., Wilson, J.W., Dive, C., Morris, I.D., Hickman,

J.A., Wakeling, A.E., Walker, P.R., Sikorska, M. (1993) EMBO J. 12, 3679–3684.
[20] Falcieri, E., Zamai, L., Santi, S., Cinti, C., Gobbi, P., Bosco, D., Cataldi, A., Betts, C., Vitale, M. (1994) Hisochemistry 102, 221–231.
[21] Oberhammer, F., Fritsch, G., Schmied, M., Pavelka, M., Printz, D., Purchio, T., Lassmann, H., Schulte-Hermann, H. (1993) J. Cell Sci. 104, 317–326.
[22] Evan, G.I., Wyllie, A.H., Gilbert, G.S., Littlewood, T.D., Land, H., Brooks, M., Waters, C.M., Penn, L.Z., Hancock, D.C. (1992) Cell 69, 119–128.
[23] Nosseri, C., Coppola, S., Ghibelli, L. (194) Exp. Cell Res. 212, 367–373.
[24] Walker, P.R., Smith, C., Youdale, T., Leblanc, J., Whitfield, J.F., Sikorska, M. (1991) Cancer Res. 51, 1078–1085.
[25] Chow, S.C., Peters, I., Orrenius, S. (1995) Exp. Cell Res. 216, 149–159.
[26] Chow, S.C., Kass, G.E., McCabe, M.J., Orrenius, S. (1992) Arch. Biochem. Biophys. 298, 143–149.
[27] Falcieri, E., Martelli, A.M., Bareggi, R., Cataldi, A., Cocco, L. (1993) Biochem. Biophys. Res. Commun. 193, 19–25.
[28] Oberhammer, F.A., Hochegger, K., Froschl, G., Tiefenbacher, R., Pavelka, M. (1994) J. Cell Biol. 126, 827–837.
[29] Filipski, J., Leblanc, J., Youdale, T., Sikorska, M., Walker, P.R. (1990) EMBO J. 9, 1319–1327.